 doi:10.20944/preprints201803.0200.v1

Article

Characterization of Porous Phosphate Coatings Created on CP Titanium Grade 2 Enriched with Calcium, Magnesium, Zinc and Copper by Plasma Electrolytic Oxidation

Krzysztof Rokosz[1], Tadeusz Hryniewicz[1,*], Raaen Steinar[2], Sofia Gaiaschi[3], Patrick Chapon[3], Winfried Malorny[4], Dalibor Matýsek[5], Łukasz Dudek[1], Kornel Pietrzak[1]

[1] Division of BioEngineering and Surface Electrochemistry, Department of Engineering and Informatics Systems, Faculty of Mechanical Engineering, Koszalin University of Technology, Racławicka 15-17, PL 75-620 Koszalin, Poland; rokosz@tu.koszalin.pl (K.R.), Tadeusz Hryniewicz (T.H.) thdhr@tu.koszalin.pl, lukasz.dudek@tu.koszalin.pl (Ł.D.), kornel.pietrzak@s.tu.koszalin.pl (K.P.)
[2] HORIBA FRANCE S.A.S., Avenue de la Vauve - Passage Jobin Yvon, CS 45002 - 91120 Palaiseau – France; sofia.gaiaschi@horiba.com, patrick.chapon@horiba.com
[3] Department of Physics, Norwegian University of Science and Technology (NTNU), Realfagbygget E3-124 Høgskoleringen 5, NO 7491 Trondheim, Norway; steinar.raaen@ntnu.no
[4] Hochschule Wismar-University of Applied Sciences Technology, Business and Design, Faculty of Engineering, DE 23966 Wismar, Germany; winfried.malorny@hs-wismar.de
[5] Institute of Geological Engineering, Faculty of Mining and Geology, VŠB—Technical University of Ostrava, 708 33 Ostrava, Czech Republic, dalibor.matysek@vsb.cz
* Correspondence: rokosz@tu.koszalin.pl; Tel.: +48-94-3478354

Abstract: In the paper, the effect of voltage increasing (from 500 V_{DC} up to 650 V_{DC}) on the structure and chemical composition of porous coating on titanium made by Plasma Electrolytic Oxidation, is presented. In the present paper, phosphates based coatings enriched with calcium, magnesium, zinc and copper in electrolyte based on 1 L of 85% concentrated H_3PO_4 with additions of $Ca(NO_3)_2{\cdot}4H_2O$, and $Mg(NO_3)_2{\cdot}6H_2O$, and $Zn(NO_3)_2{\cdot}6H_2O$, and $Cu(NO_3)_2{\cdot}3H_2O$, are described. The morphology, chemical and phase composition, are evaluated using SEM, EDS, XRD, XPS, GDOES. Based on all the analyses, it was found out that the PEO coatings are porous and enriched with calcium, magnesium, zinc and copper. They consist mainly of the amorphous phase, which is more visible for higher voltages, and it is correlated with the increasing of the total PEO coating thickness (the higher the voltage, the thicker the PEO coating). However, for 650 V_{DC} an amorphous phase and titanium substrate was also recorded with a signal from $Ti_2P_2O_7$ crystalline, that was not observed for lower voltages. It was also found out that all the obtained coatings may be divided in three sub-layers, i.e. porous, semiporous, and transition one.

Keywords: Plasma Electrolytic Oxidation (PEO); Micro Arc Oxidation (MAO); Titanium

1. Introduction

Standard electropolishing [1-4], magnetoelectropolishing [5-7] as well as high-current-density electropolishing [8-10] may be used to improve nano-scale chemical [11-13], and corrosion [3,6,14] properties of materials, as well as their surface roughness [3,15-16] and biocompatibility [17-18]. The other electrochemical treatment, known in the literature under the names of Plasma Electrolytic Oxidation (PEO) or Micro Arc Oxidation (MAO) or Spark Discharge Anodizing (SDA), may be used to form micro-porous coatings on lightweight metals, such as titanium [19-21], zirconium [22], tantalum [23], niobium [24] and their alloys (Ti6Al4V [25-26], Ti6Al7Nb [27], Ti-Nb-Zr [28], Ti-Nb-Zr-Sn [29], TNZ [30], NiTi [31]). The porous coatings obtained with such method are mostly used as biomaterials and are enriched with calcium and phosphorus to form structure similar to

 doi:10.20944/preprints201803.0200.v1

hydroxyapatite [33-35] with the addition of bactericidal zinc [36] and copper [37-38], as well as magnesium [36], which is added in case of acceleration of wound healing. Moreover, it should also be pointed out that the PEO process may be performed under DC [37-38], AC [39-40] and pulse regime [41-42], which result in coatings characterized by different porosities, as well as with different chemical composition.

2. Materials and Methods

Rectangular, titanium samples with dimensions of 10 mm x 10 mm x 2mm were treated by Plasma Electrolytic Oxidation at the voltages of 500 V_{DC}, 575 V_{DC} and 650 V_{DC} with the use of the commercial DC power supply PWR 1600H. The electrolyte composition was the following: 1 L of 85% H_3PO_4, 125 g $Ca(NO_3)_2{\cdot}4H_2O$, 125 g $Mg(NO_3)_2{\cdot}6H_2O$, 125 g $Zn(NO_3)_2{\cdot}6H_2O$, and 125 g $Cu(NO_3)_2{\cdot}3H_2O$. The SEM, EDS, XPS and GDOES measurement techniques, which have been used to characterize the PEO coatings, are described in reference [36]. The Powder X-ray diffraction (XRD) measurements were conducted using a Bruker-AXS D8 Advance instrument with the 2Θ/Θ geometry measured using a LynxEye position sensitive detector under the following conditions: radiation CuKα/Ni filter, voltage 40 kV, current 40 mA, step by step mode of 0.014 2Θ with an interval of 0.25 s per step and summation of at least five successive measurements based on the complexity of the recording. The data were processed digitally using DiffracSuite software (Bruker). Qualitative analyses of sulfates were conducted using EVA software (Bruker) and the PDF-2 database 2011 release (International Centre for Diffraction Data).

3. Results and Discussion

In **Figure 1**, the SEM images of porous coatings obtained on CP Titanium Grade 2 after PEO treatment at voltages of 500 V_{DC}, 575 V_{DC} and 650 V_{DC}, with the electrolyte consisting of 1 L of 85% concentrated phosphoric acid H_3PO_4 with 125 g calcium nitrate $Ca(NO_3)_2{\cdot}4H_2O$ and 125 g magnesium nitrate $Mg(NO_3)_2{\cdot}6H_2O$, and 125 g zinc nitrate $Zn(NO_3)_2{\cdot}6H_2O$, and 125 g copper nitrate $Cu(NO_3)_2{\cdot}3H_2O$, are presented. It can be observed that the voltage increase results in a change in surface morphology, as well pores shapes and their sharpness. On the base of EDS spectra, recorded at magnification 500 times, the atomic concentrations of Ca, Mg, Zn, Cu and P were used to calculate metals to phosphorous atomic ratios with the results presented in **Figure 2**. The PEO coating obtained at 500 V_{DC} may be characterized by Ca/P ratio, which was equal to 0.070 ± 0.009 at% (first quartile: 0.062; third quartile: 0.079), Mg/P ratio was equal 0.037 ± 0.002 at% (first quartile: 0.035; third quartile: 0.038), Zn/P ratio was equal 0.034 ± 0.006 at% (first quartile: 0.029; third quartile: 0.039), Cu/P ratio was equal 0.032 ± 0.002 at% (first quartile: 0.030; third quartile: 0.033), M/P ratio (where M=Ca+Mg+Zn+Cu) was equal 0.172 ± 0.012 at% (first quartile: 0.162; third quartile: 0.184). For PEO coatings obtained at 575 V_{DC} Ca/P ratio was equal 0.054 ± 0.002 at% (first quartile: 0.053; third quartile: 0.056), Mg/P ratio was equal 0.044 ± 0.002 at% (first quartile: 0.042; third quartile: 0.046), Zn/P ratio was equal 0.045 ± 0.003 at% (first quartile: 0.042; third quartile: 0.049), Cu/P ratio was equal 0.037 ± 0.003 at% (first quartile: 0.033; third quartile: 0.040), M/P ratio (M=Ca+Mg+Zn+Cu) was equal 0.180 ± 0.005 at% (first quartile: 0.178; third quartile: 0.184). For the PEO coatings obtained at 650 V_{DC} Ca/P ratio was equal 0.089 ± 0.011 at% (first quartile: 0.077; third quartile: 0.098), Mg/P ratio was equal 0.045 ± 0.001 at% (first quartile: 0.043; third quartile: 0.046), Zn/P ratio was equal 0.048 ± 0.005 at% (first quartile: 0.043; third quartile: 0.052), Cu/P ratio was equal 0.043 ± 0.011 at% (first quartile: 0.036; third quartile: 0.052), M/P ratio (M=Ca+Mg+Zn+Cu) was equal 0.224 ± 0.014 at% (first quartile: 0.215; third quartile: 0.236). Based on these results it can be observed that Mg/P, Zn/P, Cu/P and M/P values have positive correlation with the employed voltage. The case of Ca/P values to voltage relation can indicate different mechanism of calcium compounds in the layer. Considering standard deviation values of metal-to-phosphorous ratio it can be concluded that the most repeatable conditions of the PEO process are found at around 575 V_{DC}.

Preprints (www.preprints.org) | NOT PEER-REVIEWED | Posted: 23 March 2018 doi:10.20944/preprints201803.0200.v1

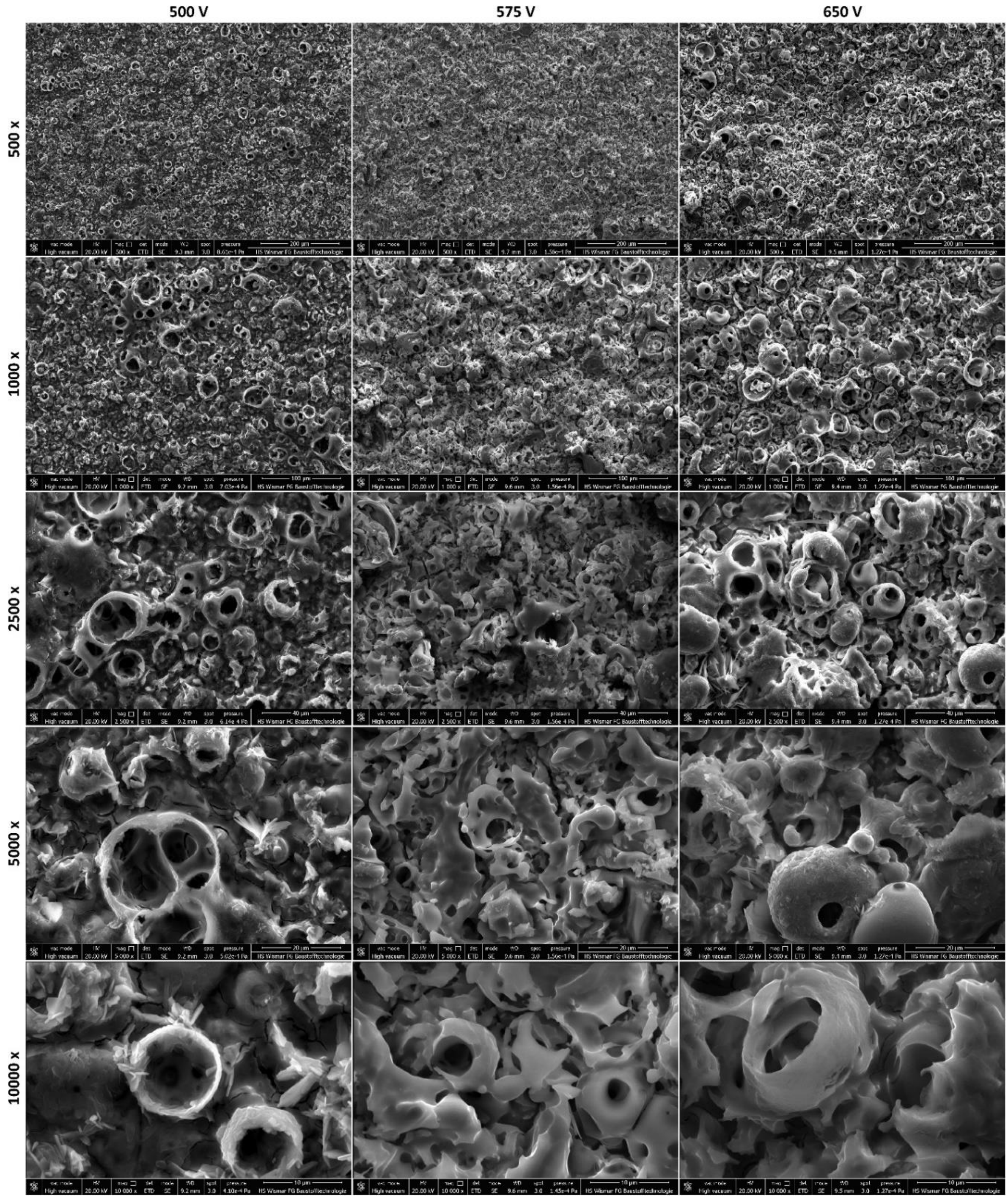

Figure 1. SEM images of coatings formed on Titanium after PEO process at voltages 500 V_{DC}, 575 V_{DC}, 650 V_{DC} in 1 L of 85% H_3PO_4 with additions of 125 $Ca(NO_3)_2{\cdot}4H_2O$, 125 g $Mg(NO_3)_2{\cdot}6H_2O$, 125 g $Zn(NO_3)_2{\cdot}6H_2O$, and 125 g $Cu(NO_3)_2{\cdot}3H_2O$ at magnifications 500, 1000, 2500, 5000, and 10000 times

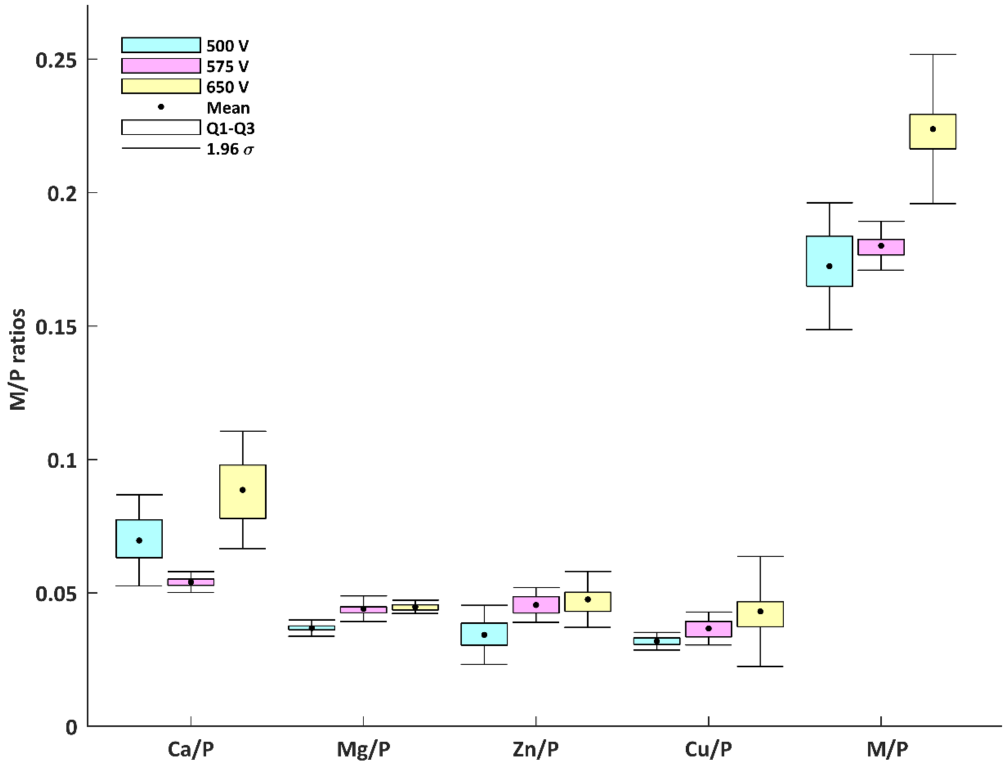

Figure 2. EDS results as Ca/P, Mg/P, Zn/P, Cu/P and M/P (M=Ca+Mg+Zn+Cu) ratios measured for coatings formed on CP Titanium Grade 2 after PEO process at the voltages 500 V_{DC}, 575 V_{DC}, 650 V_{DC} in 1 L of 85% H_3PO_4 with additions of 125 $Ca(NO_3)_2{\cdot}4H_2O$, 125 g $Mg(NO_3)_2{\cdot}6H_2O$, 125 g $Zn(NO_3)_2{\cdot}6H_2O$, and 125 g $Cu(NO_3)_2{\cdot}3H_2O$

In **Figure 3**, the XPS spectra of PEO coating formed on Titanium at the voltage of 575 V_{DC}, are presented. Based on the registered peaks, it can be stated that the top 10 nm layer of the PEO coating is enriched with calcium, magnesium, zinc, copper, titanium as well as phosphorus, oxygen and nitrogen. It should be also pointed out that carbon bounded with oxygen as well as nitrogen-oxygen compounds, should be treated as organic contaminations, which mainly origin from air and cleaning. The binding energies of 134.4eV (P2p) and 531.2 eV (O1s) may be interpreted as existing of PO_4^{3-}, or/and HPO_4^{2-}, or/and $H_2PO_4^{-}$ or/and $P_2O_7^{4-}$ groups. The Cu2p spectra with two main maxima (347.9 eV, 351 eV) as well as satellite peaks existing in the range from 939 eV up to 947 eV as well as 566.8 eV (Cu LMM) may be interpreted as Cu^{+} and Cu^{2+}, while the presence of Ca^{2+} is proved by the binding energies equal to 347.9 eV and 351.4 eV. The binding energies at 497.9 eV (Zn LMM), 500.4 eV (Zn LMM) and 1022.4 eV (Zn 2p) may suggest presence of Zn^{2+} in the PEO coating, whereas the binding energies equal to 50.6 eV (Mg2p), 89.3 eV (Mg2s), 306.8 eV (Mg KLL), indicate the presence of Mg^{2+}. The biding energy of titanium Ti2p3/2 is shifted to 460.4 eV. This can be interpreted as the presence of Ti^{4+} located in chemical compounds together within Ca^{2+}, Zn^{2+}, Mg^{2+}, Cu^{2+}, and PO_4^{3-}, or/and HPO_4^{2-}, or/and $H_2PO_4^{-}$ or/and $P_2O_7^{4-}$.

Preprints (www.preprints.org) | NOT PEER-REVIEWED | Posted: 23 March 2018 doi:10.20944/preprints201803.0200.v1

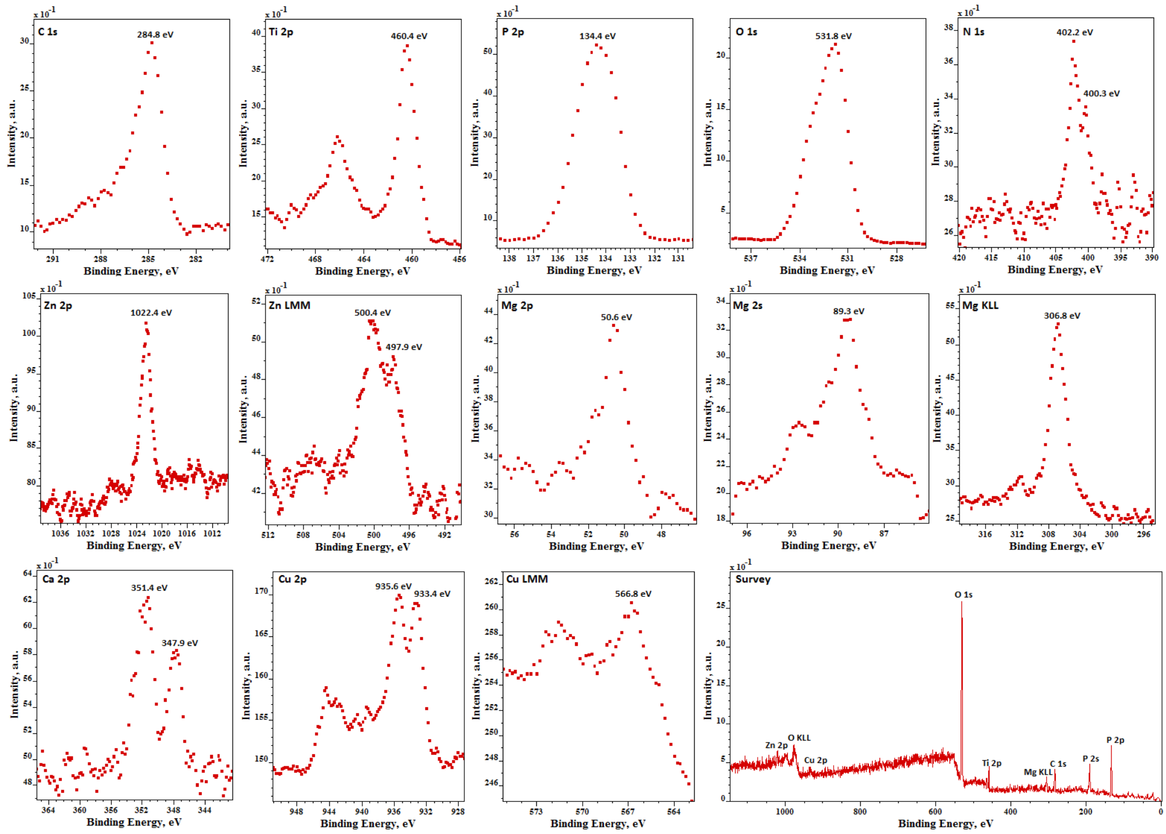

Figure 3. XPS spectra of coatings formed on CP Titanium Grade 2 after PEO process at voltage 575 V_{DC} in 1 L of 85% H_3PO_4 with additions of 125 $Ca(NO_3)_2{\cdot}4H_2O$, 125 g $Mg(NO_3)_2{\cdot}6H_2O$, 125 g $Zn(NO_3)_2{\cdot}6H_2O$, and 125 g $Cu(NO_3)_2{\cdot}3H_2O$

Figure 4 and **Figure 5** present the GDOES profile of calcium, copper, magnesium, zinc and phosphorus, oxygen, hydrogen, titanium , respectively, for PEO coatings. Based on these results it is possible to conclude that the PEO coatings may be described by a three-sub-layer model. The first porous and top sub-layers are enriched with phosphorus, oxygen, calcium, copper, magnesium and zinc. The presence of a local maximum of hydrogen and oxygen in top sub-layer, can be ascribed to surface contamination, which origins from the air and cleaning process. In the second sub-layer, which is semiporous with nested pores in the pores, a plateau is observed for all GDOES signals. Finally, in the third transition sub-layer local maxima are visible for calcium, copper, magnesium, zinc as well as in phosphorus signals. These can be interpreted as end of porosity. Based on all the GDOES spectra, one can infer that the increase of the PEO voltage results in the increase of the coating thickness.

Preprints (www.preprints.org) | NOT PEER-REVIEWED | Posted: 23 March 2018 doi:10.20944/preprints201803.0200.v1

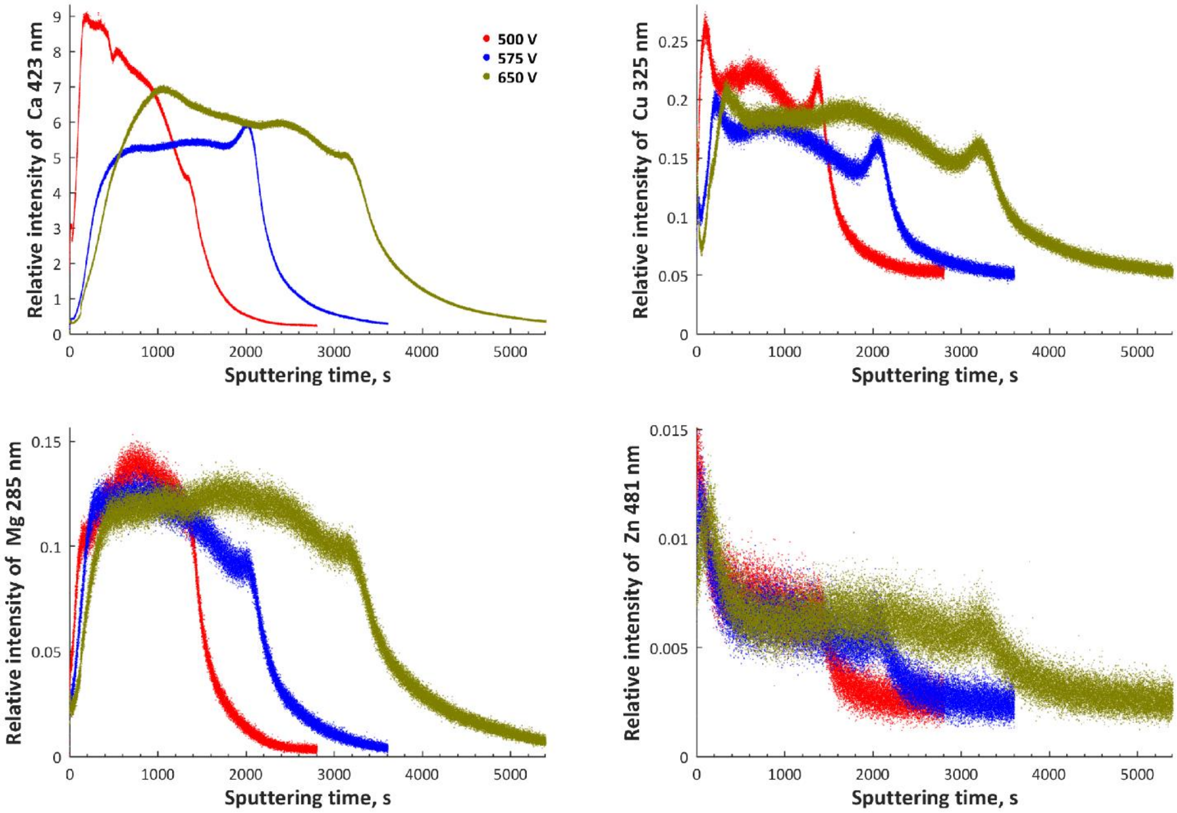

Figure 4. GDEOS (glow discharge optical emission spectroscopy) signals of calcium (Ca), magnesium (Mg), copper (Cu) and zinc (Zn) of coatings formed on CP Titanium Grade 2 after PEO process at voltages 500 V_{DC}, 575 V_{DC}, 650 V_{DC} in 1 L of 85% H_3PO_4 with additions of 125 $Ca(NO_3)_2{\cdot}4H_2O$, 125 g $Mg(NO_3)_2{\cdot}6H_2O$, 125 g $Zn(NO_3)_2{\cdot}6H_2O$, and 125 g $Cu(NO_3)_2{\cdot}3H_2O$

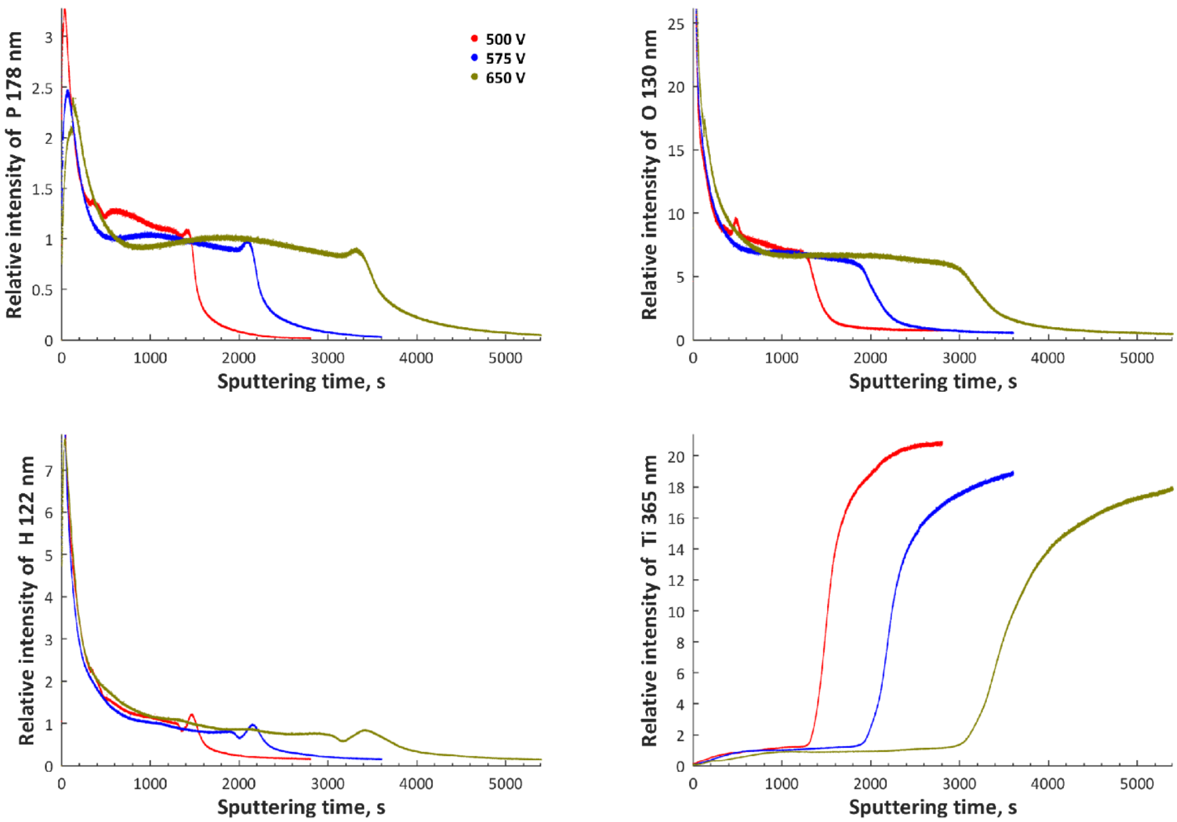

 doi:10.20944/preprints201803.0200.v1

Figure 5. GDEOS (glow discharge optical emission spectroscopy) signals of phosphorus (P), oxygen (O), hydrogen (H) and titanium (Ti) of coatings formed on CP Titanium Grade 2 after PEO process at voltages 500 V_{DC}, 575 V_{DC}, 650 V_{DC} in 1 L of 85% H_3PO_4 with the additions of 125 $Ca(NO_3)_2·4H_2O$, 125 g $Mg(NO_3)_2·6H_2O$, 125 g $Zn(NO_3)_2·6H_2O$, and 125 g $Cu(NO_3)_2·3H_2O$

The phase composition of the PEO samples was studied by XRD and results are presented in Figure 6. These results show that beyond the titanium signal coming from the substrate, the amorphous layer can be also identified. It has to be pointed out that the higher the voltage, the higher is the amorphous phase, due to the increase of the coating thickness. However, in case of PEO coating obtained at 650 V_{DC}, in addition to the amorphous phase, diffraction peaks due to the presence of $Ti_2P_2O_7$ crystals, can be observed.

Preprints (www.preprints.org) | NOT PEER-REVIEWED | Posted: 23 March 2018 doi:10.20944/preprints201803.0200.v1

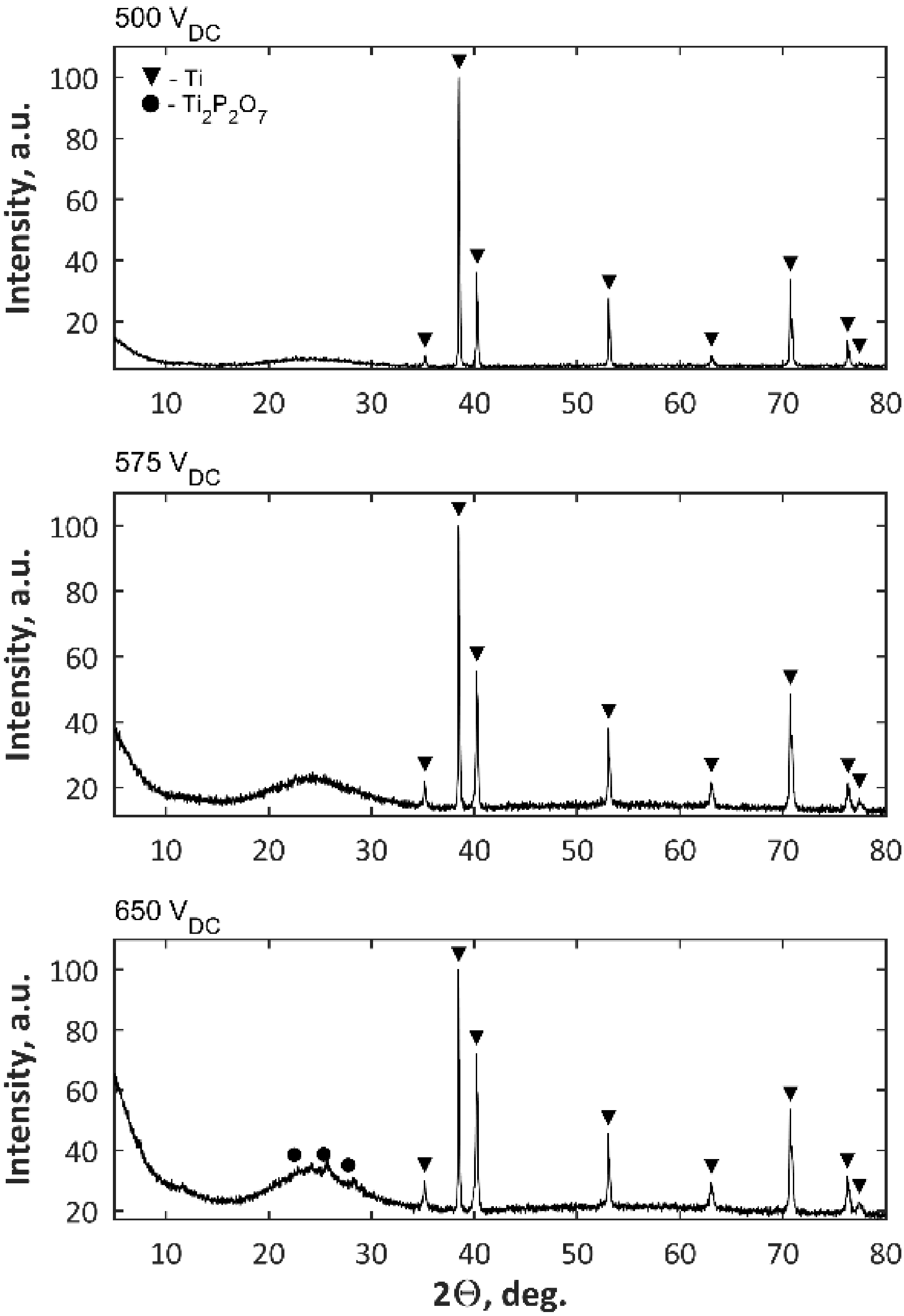

Figure 6. XRD (X-ray diffraction) patterns of coatings formed on CP Titanium Grade 2 after PEO process at voltages 500 V_{DC}, 575 V_{DC}, 650 V_{DC} in 1 L of 85% H_3PO_4 with the additions of 125 $Ca(NO_3)_2{\cdot}4H_2O$, 125 g $Mg(NO_3)_2{\cdot}6H_2O$, 125 g $Zn(NO_3)_2{\cdot}6H_2O$, and 125 g $Cu(NO_3)_2{\cdot}3H_2O$

4. Conclusions

The studies of the influence of voltage change on the chemical composition and the structure of Plasma Electrolytic Oxidation (PEO) coatings obtained on the Titanium, led to the formulation of the following conclusions:

1. the PEO process allows the formation of porous coatings enriched with phosphorus, oxygen, calcium, copper, magnesium, and zinc;

2. electrolyte containing 1 L of 85% concentrated phosphoric acid (H3PO4) with the addition of 125 g calcium nitrate $Ca(NO_3)_2{\cdot}4H_2O$, 125 g magnesium nitrate $Mg(NO_3)_2{\cdot}6H_2O$, 125 g zinc nitrate $Zn(NO_3)_2{\cdot}6H_2O$, and 125 g copper nitrate $Cu(NO_3)_2{\cdot}3H_2O$ can be successfully used for PEO treatment of titanium;

3. the higher the PEO voltage, the thicker the PEO coating, i.e. the thickest coating was obtained at 650 V_{DC} and the thinnest one at 500 V_{DC};

4. The higher the voltage, the thicker the coating, that's why from XRD there is a stronger amorphous signal. the presence of a $Ti_2P_2O_7$ crystalline phase was recorded only for the highest voltage, i.e. 650 V_{DC};

5. the obtained PEO coatings can be described using a three sub-layers model, i.e. the top, porous one (contaminated with carbon-nitrogen-oxygen compounds originated from the air and cleaning process), semiporous one (enriched in phosphorus, oxygen, calcium, copper, magnesium, zinc, and depleted in titanium), transition one (increasing of the amount of titanium, while the decreasing the amounts of phosphorus, oxygen, calcium, copper, magnesium, and zinc;

6. the top 10 nm of porous coating most likely is constructed of titanium (Ti4^{+}), calcium (Ca^{2+}), magnesium (Mg^{2+}), zinc (Zn^{2+}), copper (Cu^{2+} and Cu^{+}), and phosphates (PO_4^{3-} and/or HPO_4^{2-}, and/or $H_2PO_4^{-}$, and/or $P_2O_7^{4-}$).

Acknowledgments: This work was supported by a subsidy from Grant OPUS 11 of National Science Centre, Poland, with registration number 2016/21/B/ST8/01952, titled "Development of models of new porous coatings obtained on titanium by Plasma Electrolytic Oxidation in electrolytes containing phosphoric acid with addition of calcium, magnesium, copper and zinc nitrates".

Author Contributions: Krzysztof Rokosz and Tadeusz Hryniewicz conceived and designed the experiments; Krzysztof Rokosz, Sofia Gaiaschi, Patrick Chapon, Steinar Raaen, Dalibor Matýsek and Winfried Malorny performed the experiments; Krzysztof Rokosz, Tadeusz Hryniewicz, Łukasz Dudek, and Kornel Pietrzak analyzed the data; Krzysztof Rokosz, Tadeusz Hryniewicz, Łukasz Dudek and Kornel Pietrzak contributed reagents, materials, analysis tools; Krzysztof Rokosz and Tadeusz Hryniewicz wrote the paper.

Conflicts of Interest: Declare conflicts of interest or state "The authors declare no conflict of interest." Authors must identify and declare any personal circumstances or interest that may be perceived as inappropriately influencing the representation or interpretation of reported research results. Any role of the funding sponsors in the design of the study; in the collection, analyses or interpretation of data; in the writing of the manuscript, or in the decision to publish the results must be declared in this section. If there is no role, please state "The founding sponsors had no role in the design of the study; in the collection, analyses, or interpretation of data; in the writing of the manuscript, and in the decision to publish the results".

References

1. Lochynski P., Sikora A., Szczygieł B., Surface morphology and passive film composition after pickling and electropolishing, *Surf. Eng.* 33 (2017) 395-403.
2. Lochynski P., Kowalski M., Szczygieł B., Kuczewski K., Improvement of the stainless steel electropolishing process by organic additives, *Pol. J. Chem. Technol.* 18(4) (2016) 76-81.
3. Rokosz K., Electrochemical Polishing in Magnetic Field, first ed., Koszalin University of Technology Publishing House, Koszalin, 2012, Monograph No 219; ISSN 0239-7129. (In Polish)
4. Hryniewicz T., Rokicki R., Rokosz K., Co-Cr alloy corrosion behaviour after electropolishing and "magnetoelectropolishing" treatments, *Surf. Coat. Technol.* 62 (2008) 3073–3076.
5. Hryniewicz T., Rokosz K., Polarization characteristics of magnetoelectropolishing stainless steels, *Mater. Chem. Phys.* 122 (2010) 169–174.
6. Hryniewicz T., Rokosz K. , Corrosion resistance of magnetoelectropolished AISI 316L SS biomaterial, *Anti-Corros. Methods Mater.* 61 (2014) 57–64.
7. Rokosz K., Hryniewicz T., XPS measurements of LDX 2101 duplex steel surface after magnetoelectropolishing. *Int. J. Mater. Res.* 104 (2013) 1223–1232.
8. Rokosz K., Hryniewicz T., Simon F., Rzadkiewicz S., Comparative XPS analysis of passive layers composition formed on AISI 304L SS after standard and high-current density electropolishing, *Surf. Interface Anal.* 47 (2015) 87–92.
9. Rokosz K., Lahtinen J., Hryniewicz T., Rzadkiewicz S., XPS depth profiling analysis of passive surface layers formed on austenitic AISI 304L and AISI 316L SS after high-current-density electropolishing, *Surf. Coat. Technol.*, 276 (2015) 516–520.
10. Rokosz K., Hryniewicz T., Rzadkiewicz S., Raaen S., High-Current-Density Electropolishing (HDEP) of AISI 316L (EN 1.4404) Stainless Steel, *Teh. Vjesn. Tech. Gaz.* 22(2) (2015) 415-424.
11. Rokosz K., Hryniewicz T., Raaen S., Cr/Fe ratio by XPS spectra of magnetoelectropolished AISI 316L SS fitted by Gaussian-Lorentzian shape lines, *Teh. Vjesn. Tech. Gaz.* 21 (2014) 533–538.
12. Hryniewicz T., Konarski P., Rokicki R., Valíček J., SIMS analysis of hydrogen content in near surface layers of AISI 316L SS after electrolytic polishing under different conditions, *Surf. Coat. Technol.* 205 (2011) 4228–4236.
13. Rokosz K., Hryniewicz T.; Raaen S., Characterization of passive film formed on AISI 316L stainless steel after magnetoelectropolishing in a broad range of polarization parameters, *Steel Res. Int.* 83 (2012) 910–918.
14. Hryniewicz T., Rokicki R., Rokosz K., Corrosion and surface characterization of titanium biomaterial after magnetoelectropolishing, *Surf. Coat. Technol.* 203 (2008) 1508–1515.
15. Valíček J., Drzik M., Hryniewicz T., Harničarova M., Rokosz K., Kusnerova M., Barcova K., Brazina D., Noncontact method for surface roughness measurement after machining, *Meas. Sci. Rev.* 12 (2012) 184–188.
16. Kusnerova M., Valíček J., Harničarova M., Hryniewicz T., Rokosz K., Palkova Z., Vaclavik V., Repka M., Bendova M.A., proposal for simplifying the method of evaluation of uncertainties in measurement results, *Meas. Sci. Rev.* 13 (2013) 1–6.
17. Rokicki R., Hryniewicz T., Pulletikurthi C., Rokosz K., Munroe N., Towards a Better Corrosion Resistance and Biocompatibility Improvement of Nitinol Medical Devices, *J. Mater. Eng. Perform.*, 24(4) (2015) 1634-1640.
18. Hryniewicz T., Rokicki R., Rokosz K., Magnetoelectropolished Titanium Biomaterial, in R. Pignatello (Eds.), *Biomaterials Science and Engineering*, InTech, London, 2011, pp. 227–248.
19. Wang Y., Jiang B., Lei T., Guo L., Dependence of growth features of microarc oxidation coatings of titanium alloy on control modes of alternate pulse, *Mater. Lett.* 58 (2004) 1907–1911.
20. Rokosz K., Hryniewicz T., Dudek Ł., Matysek D., Valíček J., Harničarova M., SEM and EDS analysis of surface layer formed on titanium after plasma electrolytic oxidation in H_3PO_4 with the addition of $Cu(NO_3)_2$, *J. Nanosci. Nanotechnol.* 16 (2016) 7814–7817.
21. Rokosz K., Hryniewicz T., Matysek D., Raaen S., Valíček J., Dudek Ł., Harničarova M., SEM, EDS and XPS analysis of the coatings obtained on titanium after plasma electrolytic oxidation in electrolytes containing copper nitrate, *Materials* 9 (2016) 1-12.
22. Sowa M., Lastowka D., Kukharenko A.I., Korotin D.M., Kurmaev E.Z., Cholakh S.O., Simka W., Characterisation of anodic oxide films on zirconium formed in sulphuric acid: XPS and corrosion resistance investigations, *J. Solid State Electrochem.*21(1) (2017) 203-210.

23. Rokosz K., Hryniewicz T., Chapon P., Raaen S., Sandim H.R.Z., XPS and GDOES characterisation of porous coating enriched with copper and calcium obtained on Tantalum via Plasma Electrolytic Oxidation, *J. Spectrosc.* 2016 (2016) 7093071.
24. Rokosz K., Hryniewicz T., Comparative SEM and EDX analysis of surface coatings created on niobium and titanium alloys after Plasma Electrolytic Oxidation (PEO), *Teh. Vjesn. Tech. Gaz*. 24 (2017) 465–472.
25. Krząkała A., Młyński J., Dercz G., Michalska J., Maciej A., Nieużyła L., Simka W., Modification of Ti-6Al-4V alloy surface by EPD-PEO process in $ZrSiO_4$ suspension, *Arch. Metall. Mater*. 59 (2014) 199–204.
26. Rokosz K., Hryniewicz T., Raaen S., Development of Plasma Electrolytic Oxidation for improved Ti6Al4V biomaterial surface properties, *Int. J. Adv. Manuf. Technol*. 85 (2016) 2425–2437.
27. Simka W., Nawrat G., Chlode J., Maciej A., Winiarski A., Szade J., Radwanski K., Gazdowicz J., Electropolishing and anodic passivation of Ti6Al7Nb alloy, *Przem. Chem*. 90 (2011) 84–90.
28. Rokosz K., Hryniewicz T., Raaen S., Chapon P., Development of copper-enriched porous coatings on ternary Ti-Nb-Zr alloy by Plasma Electrolytic Oxidation, Int. *J. Adv. Manuf. Technol*. 89 (2017) 2953–2965.
29. Rokosz K., Hryniewicz T., Raaen S., Chapon P., Investigation of porous coatings obtained on Ti-Nb-Zr-Sn alloy biomaterial by Plasma Electrolytic Oxidation: Characterisation and Modelling, *Int. J. Adv. Manuf. Technol*. 87 (2016) 3497–3512.
30. Rokosz K., Hryniewicz T., Characteristics of porous and biocompatible coatings obtained on Niobium and Titanium-Niobium-Zirconium (TNZ) alloy by Plasma Electrolytic Oxidation, *Mechanik* 12 (2015) 15–18.
31. Rokosz K., Hryniewicz T., Raaen S., SEM, EDS and XPS analysis of nanostructured coating obtained on NiTi biomaterial alloy by Plasma Electrolytic Oxidation (PEO), Teh. Vjesn. Tech. Gaz. 24 (2017), 193–198.
32. Simka W., Sadowski A., Warczak M., Iwaniak A., Dercz G., Michalska J., Maciej A., Modification of titanium oxide layer by calcium and phosphorus, *Electrochim. Acta* 56 (2011) 8962–8968.
33. Rokosz K., Hryniewicz T., Gaiaschi S., Chapon P., Raaen S., Pietrzak K., Malorny W., Characterisation of calcium- and phosphorus-enriched porous coatings on CP Titanium Grade 2 fabricated by plasma electrolytic oxidation, *Metals* 7 (2017) 1-17.
34. Rokosz K., Hryniewicz T., Malorny W., Characterisation of porous coatings obtained on materials by Plasma Electrolytc Oxidation, *Mater. Sci. Forum* 862 (2016) 86–95.
35. Rokosz K., Hryniewicz T., Pietrzak K., Sadlak P., Valíček J., Fabrication and characterisation of porous, calcium enriched coatings on titanium after Plasma Electrolytic Oxidation under DC regime, *Adv. Mater. Sci*. 17 (2017) 55–67.
36. Rokosz K., Hryniewicz T., Gaiaschi S., Chapon P., Raaen S., Pietrzak K., Malorny W., Fernandes J.S., Characterization of Porous Phosphate Coatings Enriched with Magnesium or Zinc on CP Titanium Grade 2 under DC Plasma Electrolytic Oxidation, *Metals* 8 (2018) 1-13.
37. Rokosz K., Hryniewicz T., Raaen S., Chapon P., Dudek Ł., GDOES, XPS and SEM with EDS analysis of porous coatings obtained on Titanium after Plasma Electrolytic Oxidation, *Surf. Interface Anal*. 49 (2016) 303–315.
38. Rokosz K., Hryniewicz T., Raaen S., Malorny W., Fabrication and characterization of porous coatings obtained by Plasma Electrolytic Oxidation, *J. Mech. Energy Eng*. 1 (2017) 23–30.
39. Aliasghari S., Němcová A., Skeldon P., G.E. Thompson , Influence of coating morphology on adhesive bonding of titanium pre-treated by plasma electrolytic oxidation, *Surf. Coat. Technol*. 289 (2016) 101–109.
40. Gnedenkov S.V., Sharkeev Y.P., Sinebryukhov S.L., Khrisanfova O.A., Legostaeva E.V., Zavidnaya A.G., Puz’ A.V., Khlusov I.A., Opra D.P., Functional coatings formed on the titanium and magnesium alloys as implant materials by plasma electrolytic oxidation technology: Fundamental principles and synthesis conditions, *Corros. Rev*. 34(1–2) (2016) 65–83.
41. Hariprasad S., Ashfaq M., Arunnellaiappan T., Harilal M., Rameshbabu N., Role of electrolyte additives on in-vitro corrosion behavior of DC plasma electrolytic oxidization coatings formed on CP-Ti, *Surf. Coat. Technol*. 292 (2016) 20–29.
42. Huang Q., Elkhooly T.A., Liu X., Zhang R., Yang X., Shen Z., Feng Q., Effects of hierarchical micro/nano-topographies on the morphology, proliferation and differentiation of osteoblast-like cells, *Colloid Surf. B-Biointerfaces* 145 (2016)37–45.
43. Casa Software Ltd. CasaXPS: Processing Software for XPS, AES, SIMS and More, 2018., http://www.casaxps.com, (accessed 25 February 2018).

 doi:10.20944/preprints201803.0200.v1

44. Wagner C.D., Naumkin A.V., Kraut-Vass A., Allison J.W., Powell C.J., Rumble J.R., NIST Standard Reference Database 20, Version 4.1. Available online: http://srdata.nist.gov/xps, 2012, (accessed 25 February 2018).
45. Nelis T., Payling R., *Practical Guide to Glow Discharge Optical Emission Spectroscopy*; RSC Analytical Spectroscopy Monographs, Royal Society of Chemistry, Cambridge, 2002.
46. *Pulsed RF Glow Discharge Optical Emission Spectrometry*; Ultra Fast Elemental Depth Profiling, HORIBA Jobin Yvon, Paris, France, 2014, Available online: http://www.horiba.com/scientific/products/atomic-emissionspectroscopy/glow-discharge, (accessed 25 February 2018).
47. DiP: Differential Interferometry Profiling; HORIBA Jobin Yvon: Paris, France, 2015, Available online: http://www.horiba.com/fileadmin/uploads/Scientific/Documents/GDS/HJY_BRO_GDOES_DiP.pdf, (accessed 25 February 2018).
48. Author 1, A.; Author 2, B. Title of the chapter. In *Book Title*, 2nd ed.; Editor 1, A., Editor 2, B., Eds.; Publisher: Publisher Location, Country, 2007; Volume 3, pp. 154–196, ISBN.
49. Author 1, A.; Author 2, B. *Book Title*, 3rd ed.; Publisher: Publisher Location, Country, 2008; pp. 154–196, ISBN.
50. Author 1, A.B.; Author 2, C. Title of Unpublished Work. *Abbreviated Journal Name stage of publication* (under review; accepted; in press).
51. Author 1, A.B. (University, City, State, Country); Author 2, C. (Institute, City, State, Country). Personal communication, 2012.
52. Author 1, A.B.; Author 2, C.D.; Author 3, E.F. Title of Presentation. In Title of the Collected Work (if available), Proceedings of the Name of the Conference, Location of Conference, Country, Date of Conference; Editor 1, Editor 2, Eds. (if available); Publisher: City, Country, Year (if available); Abstract Number (optional), Pagination (optional).
53. Author 1, A.B. Title of Thesis. Level of Thesis, Degree-Granting University, Location of University, Date of Completion.
54. Title of Site. Available online: URL (accessed on Day Month Year).